A Robust and Effective GNSS/INS Integration Optimizing Cost and Effort

Michael Felux[1,2], Markus Rippl[1], Anja Grosch[1]

([1] German Aerospace Center (DLR), Munich, Germany
[2] Technische Universität München, Munich, Germany)
(Email: michael.felux@dlr.de)

Meeting all requirements for flying approaches in bad weather conditions is one of the most demanding and challenging aspects of present day airborne navigation. Stand-alone satellite navigation has not yet reached the point of being sufficiently robust and accurate in order to reach certification level. Therefore, in this work the performance of an integrated satellite/inertial navigation system (GNSS/INS) is investigated in order to cope with short term losses of GNSS signals. We consider a low-cost Micro Electronic Mechanical System (MEMS) INS which is constantly reinitialized with information coming solely from GNSS. It takes over navigational responsibility when a loss of signal occurs or other failures in the satellite navigation system are detected. For the GNSS to provide all information necessary to initialize an INS, a minimum of three antennas is needed to measure the aircraft's attitude along with its speed and position. Error models for positioning, speed and attitude estimation are used to create a model for initialization uncertainties. Together with error models for the accelerometers and gyros in the Inertial Measurement Unit (IMU), the behavior of the whole proposed architecture is determined via performance simulations. As a maximum allowable error 15.3 meters (which corresponds to the CAT III horizontal alert limit for GNSS approaches) are taken. Our simulations show that this limit is not exceeded for at least 14 seconds after the take-over of navigational responsibility by the INS.

KEY WORDS

1. GNSS   2. INS integration   3. Continuity improvement

1. INTRODUCTION AND DEFINITION OF TERMS   Flying approaches in low visibility conditions is the remaining challenge today when relying on satellite navigation in aviation. Very stringent requirements are imposed when safety critical issues, like landing an airplane, are involved.

One of the biggest threats to continuity of the service is a loss of signal from one or more satellites, especially if the number of visible satellites is low. This can be the case during a maneuver where the antenna points away from satellites which were previously used for navigation. Mountains surrounding an airport or airports in polar regions with limited satellite visibility can increase this problem. Figure 1 shows the number of tracked satellites in a tight curve during a flight test performed in 2008 by the Institute of Communications and

Navigation at the Technische Universität München. The ground track of the flight path is shown in figure 2.
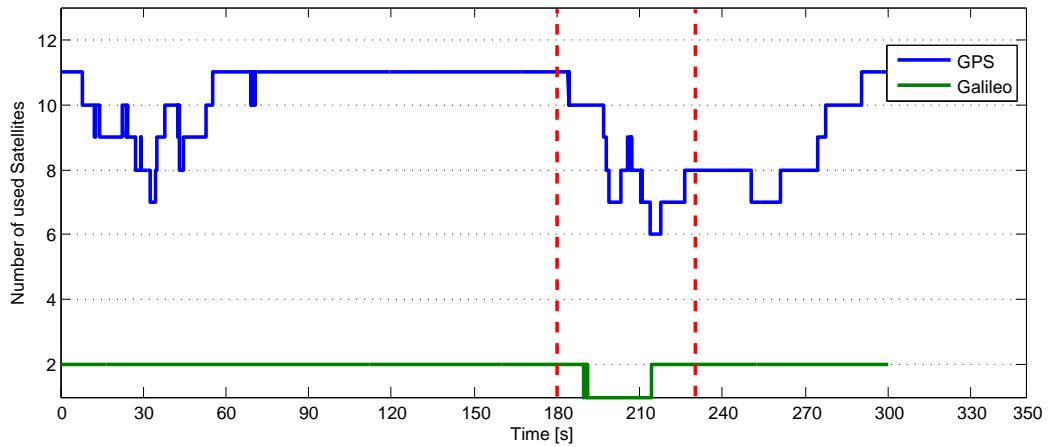

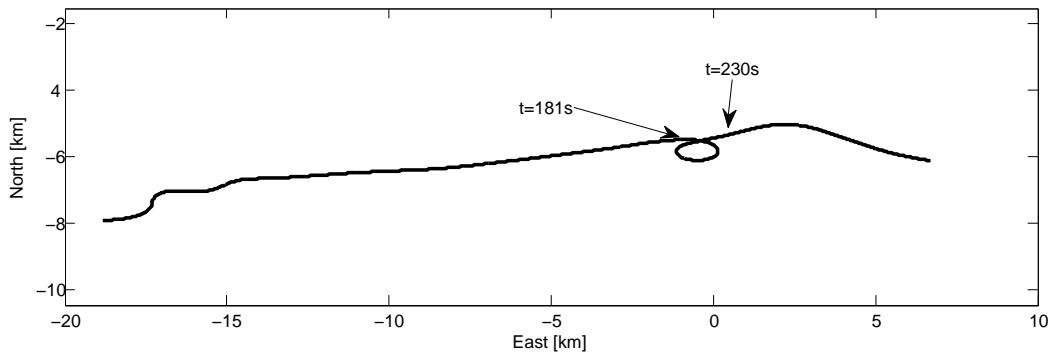Figure 1: Number of visible satellites during the maneuver shown in figure 2

Figure 2: North-East plot of the flight track

Although in this example there were enough satellites visible for navigational purposes throughout the whole maneuver, it still shows quite well the problem which can arise when satellite coverage is less favorable. The occurring outages of satellite tracking are typically rather short, however, and can therefore be bridged by the use of an Inertial Navigation System (INS). Since it is not intended to rely on inertial navigation for a long period of time, low-cost Micro Electronical Mechanical System (MEMS) sensors can be used. They are not very stable and drift rather quickly. However, during the time needed for reacquisition of the GNSS signal the accuracy is sufficient as is shown later in section 4.

2. INITIALIZATION AND NAVIGATION WITH INS   The idea of inertial navigation is based on Newton's Laws. The INS integrates measured specific forces and turn rates over time. Based on this information and initial parameters it derives current position estimates. In

formulas this can be written as

$$x(t) = x_0 + \int_{t_0}^{t} v(t)dt = x_0 + \int_{t_0}^{t} \left[v_0 + \int_{\tau_0}^{\tau} a(t)d\tau \right] dt \tag{1}$$

where $x(t)$ denotes the position to be estimated, x_0 an initial position, v_0 and $v(t)$ an initial and time depending speed, respectively, a the acceleration and the timespan from t_0 to t the timespan during which the INS is used. Basically INS can be divided into two different groups, namely gimbaled gyro-stabilized platforms and strap-down systems. In aviation, the latter is mostly used due to lower costs, reduced size and weight and greater reliability [1]. However, in comparison to the gimbaled system the measurements are not isolated from the rotational motion of the vehicle, i.e. the accelerations and turn rates are measured in the aircraft's body frame. If the attitude in space is known, the position in the navigation frame (i.e. in north, east and down direction) can be obtained simply through multiplication with the corresponding transformation matrix. An initial attitude has to be known while information about attitude changes is obtained through integration of the measured turn rates. But there are still more factors which influence the measurements and therefore have to be considered. Newton's laws are only valid in inertial reference frames, however, the navigation frame is moving and rotating. Hence, what is measured in the IMU is a lot more than the actual accelerations created by movements of the plane. Measured but unwanted specific forces arise due to Coriolis and Centripetal Acceleration. The first one is caused by the aircraft being a moving body in a rotating earth-reference frame, while the latter one is mainly caused by the rotation of the earth. Another very obvious nuisance parameter is the earth's gravitational acceleration. It has to be compensated by using a precise gravitation model depending on current position. When all these issues are addressed and the measured specific forces in the body-frame f^b are transformed to the navigation frame by the rotation matrix C_b^n containing information about the aircraft's Euler angles, the true acceleration can be written as

$$\boldsymbol{a} = \dot{\boldsymbol{v}} = C_b^n \boldsymbol{f}^b - [2\boldsymbol{\omega}_{ie} + \boldsymbol{\omega}_{en}] \times \boldsymbol{v}_e^n - \boldsymbol{g}_l^n \tag{2}$$

with $\boldsymbol{\omega}_{ie}$ and $\boldsymbol{\omega}_{en}$ the turn rate of the earth with respect to the inertial frame and the turn rate of the navigation frame with respect to the earth frame, respectively. $\boldsymbol{v}_e^n$ and $\boldsymbol{g}_l^n$ are speed with respect to the earth (ground speed) and the local gravitation vector, both in navigational coordinates. The $\times$ operator shall denote the cross product.

3. OBTAINING THE INITIAL VALUES   As described in the previous section, initial position, speed and attitude information have to be available to initialize an INS. All these input parameters can be obtained from GNSS measurements:

(a) Positioning is assumed to be done by GNSS positioning augmented with GBAS corrections. Errors for this method are typically in the decimeter range [2].

(b) The velocity of the aircraft can be estimated very precisely through measurements of the Doppler-shift in the carrier frequency of the signal. Errors for this method usually are in the millimeter to centimeter per second range [3].

(c) Attitude determination with at least three antennas can also be achieved through carrier phase measurements. The exact method is very well described in literature such as [4]. Accuracies of about $0.1°$ can be achieved with this method [5].

The following table 1 gives an overview of the assumed standard deviations of the errors in the simulation. All of them are considered to be Gaussian distributed with zero mean. It can be expected that the imperfect measurements from GNSS, together with the imperfect low-cost inertial sensors will cause the navigation system's position solution to drift away from the real position. On this account, this work investigates the timespan during which the position error remains below a certain threshold value.

Error type	Standard Deviation
Initial position	$0.5m$ in each direction
Initial speed horizontally	$0.004 \frac{m}{s}$
Initial speed vertically	$0.01 \frac{m}{s}$
Initial attitude horizontally	$0.1°$
Initial attitude vertically	$0.15°$

Table 1: Standard deviations of errors in initial values used for simulation

4. MODELING AND SIMULATION OF THE ERRORS   According to [6] the erroneous sensor output s for accelerometers and rate gyros can generally be described by an offset due to a scaling factor s_f and a bias term $b(t)$ while s_t is the true value to be measured.

$$s = (1 + s_f)s_t + b(t)$$

The bias term consists of a constant null-shift b_0, a time varying bias term $b_1(t)$ and a sampling noise term $b_w(t)$.

$$b(t) = b_0 + b_1(t) + b_w(t) \tag{3}$$

Values for s_f and b_0 can either be determined through calibration measurements or are estimated in real time. Therefore, they shall be neglected in the simulation since they can be assumed to be known. The $b_1(t)$-term is modeled as a Gauss-Markov-Process described though a time constant τ and white driving process noise with variance ω_{b_1} as

$$\dot{b_1}(t) = -\frac{1}{\tau}b_1(t) + \omega_{b_1} \tag{4}$$

Table 2 summarizes the simulated standard deviations for the IMU. With this model the measured specific force $\boldsymbol{f^b}$ and the transformation matrix C_b^n from equation (2) are fully described. For simplicity the user was assumed to be stationary. Hence, every movement and attitude change is a direct result of erroneous sensor outputs. The $\boldsymbol{\omega}_{ie}$-term from equation (2) depends on the user's latitude. It has been simulated as constant since the aircraft's latitude would only change insignificantly in the analyzed time frame. $\boldsymbol{\omega}_{en}$ depends on current speed as well as latitude. Again, the latitude dependency shall be neglected for the same reasons as before.

The speed $\boldsymbol{v}_e^n$ changes throughout the simulation due to acceleration and attitude errors and, therefore, has to be considered.

The gravitational acceleration vector $\boldsymbol{g}_l^n$ consists of two parts. The first one is gravitational acceleration through mass attraction, the second one is centripetal acceleration through earth rotation. Gravitational acceleration is not constant and derived from a mapping function. Centripetal acceleration also depends on latitude and altitude above the earth. However, the influence of absolute position errors due to wrong measurements is again negligibly small

and thus no gravitational errors or corrections have been simulated. The whole navigation problem can now be rewritten as an Ordinary Differential Equation (ODE) in the form $\dot{y} = f(t, y)$ with initial values $y(t_0) = y_0$ and then becomes:

$$
\begin{pmatrix} \mathbf{q} \\ \mathbf{x} \\ \dot{\boldsymbol{x}} \\ b_1 \\ b_2 \end{pmatrix}' = \begin{pmatrix} b_1 + \omega_{b_1} \\ \dot{x} \\ C_b^n \cdot (\boldsymbol{f}^b + b_2 + \omega_{b_2}) - 2\boldsymbol{\omega}_{ie} + \boldsymbol{\omega}_{en} \times \boldsymbol{v}_e^n \\ -\frac{1}{\tau} b_1(t) + \omega_{b_1} \\ -\frac{1}{\tau_2} b_2(t) + \omega_{b_2} \end{pmatrix} \tag{5}
$$

with initial conditions

$$
y(t_0) = \begin{pmatrix} \boldsymbol{q_0} \\ \boldsymbol{x_0} \\ \dot{\boldsymbol{x_0}} \\ 0 \\ 0 \end{pmatrix}
$$

where $\mathbf{q}$ is the aircraft's attitude, $\mathbf{x}$ the position, $\dot{\boldsymbol{x}}$ the acceleration, b_1 and b_2 the bias term for acceleration and the gyros, respectively, all as described in the previous paragraphs. The following simulations are based on this equation.

Error type	Standard Deviation
Driving process noise (gyros)	$0.05°/s$
Sampling noise (gyros)	$0.05°/s$
Driving process noise (accelerometers)	$0.001g$
Sampling noise (accelerometers)	$0.001\ g$

Table 2: Standard deviations of noise in the IMU

An important mathematical detail is the random noise process of in the bias terms b_1. This makes equation (5) a stochastic differential equation. What is of interest in this context is the behavior of equation (4) which is of the form

$$
\frac{dx}{dt} = c \cdot b(x) + \sigma(x)\xi
$$

where $\sigma(x)$ is the amplitude and ξ is white noise. This white noise is considered as time derivative of a Wiener process (or Brownian motion) as described for example in [7]. The Wiener process has the property that it has a Gaussian distribution given by

$$
g(t) = \frac{1}{\sigma\sqrt{2\pi \cdot t}} e^{-\frac{1}{2}\left(\frac{x}{\sigma\sqrt{t}}\right)^2}
$$

and thus is dependent on time. It is obvious from this equation that the standard deviation of the process is $\sigma\sqrt{t}$.

This fact has to be considered when solving problem (5) numerically. The random variable generated in each time step of the discretization has to be scaled by a factor $\tau^{-\frac{1}{2}}$ where τ is the step size of the integration.

5. OVERALL PERFORMANCE SIMULATION   For overall performance the simulations are run with the full range of possible errors summarized in tables 1 and 2. They were all assumed

to be independent from each other. To obtain some statistical reliability 1000 simulation runs for each scenario are performed. As initial parameters a non moving and unaccelerated user is assumed at the DLR site in Oberpfaffenhofen, at 48°04.88'N, 11°16.98'E at an altitude of 1000m. It is also assumed that in the beginning the body and navigation frame were fully aligned. With a simulated three dimensional speed of $[0, 0, 0]^T$ the true trajectory would just be a steady point. Every deviation from this is due to imperfect measurements and performance of the system.

Figure 3 shows the results for the complete range of errors horizontally in the first plot and vertically in the second one. Plotted on the x-axis is the time in seconds and on the y-axis the absolute value of the error in meters. The allowable alert limits for the different approach categories are shown.

The first very obvious fact is that the horizontal error is much larger than the vertical one and the trajectories drift apart a lot faster. This is due to geometric reasons. Small angular perturbations have a much larger effect in the directions perpendicular to the true specific force vector than along its direction.

Simple geometric calculations show that the error perpendicular to the specific force is about 100 times larger than the error along the specific force for error uncertainties of 0.06°. This corresponds exactly to what can be seen in the error histograms in figure 4. None of the north, east or down error components are Gaussian distributed although the shape of the histogram (4b) may suggest this. This result has been derived with the Jarque-Bera test [8] at a significance level of 10%.

The overall behavior is as expected. Most of the trajectories keep drifting the further away from the true position, the longer the simulation is run. After 20 seconds, a mean horizontal error of 14 meters is reached. The maximum error encountered was 48.3 meters while the minimum error was just 0.38 meters. Some trajectories show increasing errors at the beginning and then they approach the true position again, others stay rather close to zero over the whole simulated timespan. This is not surprising either, since the random process of the errors in the accelerometers and gyros can change its behavior and thus the direction in which the error is drifting. Hence the solution can drift away initially, converge back to the true value and eventually become worse again. The smallest error after 20 seconds is therefore not a very meaningful value since it can be expected that the error would start drifting to another direction if the simulation was continued.

In the context of aviation the interesting question is how long a pilot can rely on information from the INS in case of a GNSS outage. From figure 3 it can be seen that in the case of CAT I it takes 19.5 seconds until the first trajectory exceeds the horizontal alert limit (HAL) of 40 meters. In case of CAT II and CAT III the time where the INS delivers reliable information is still 14.4 and 14 seconds, respectively. It is interesting to note that the vertical alert limit (VAL) even in CAT III conditions is never exceeded throughout the simulation time. As mentioned above this is due to the always present gravitational acceleration which is (at least in civil aviation) large compared to Centripetal or other accelerations caused by the movement of the aircraft.
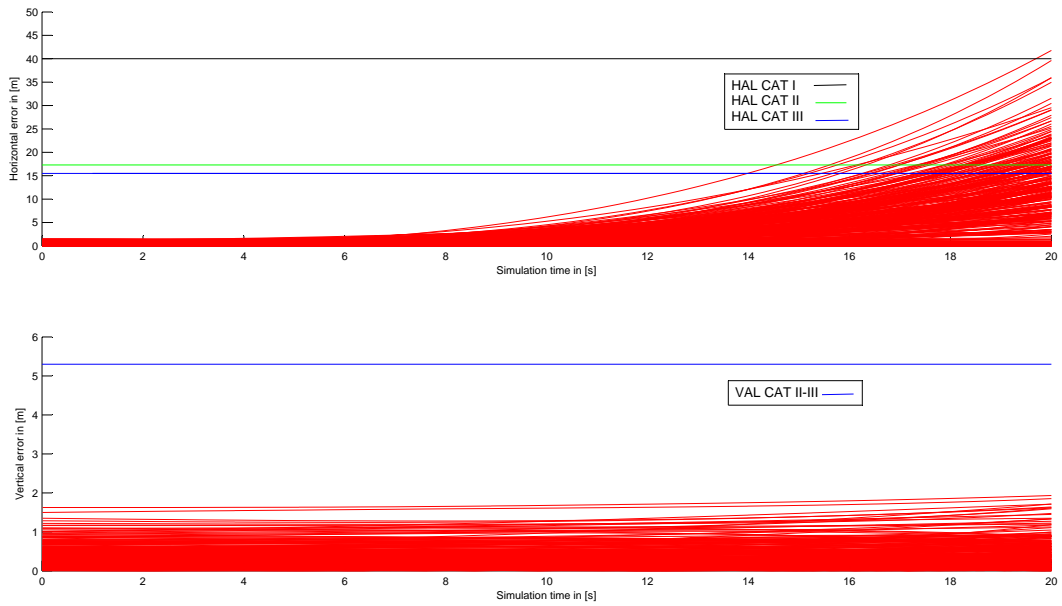
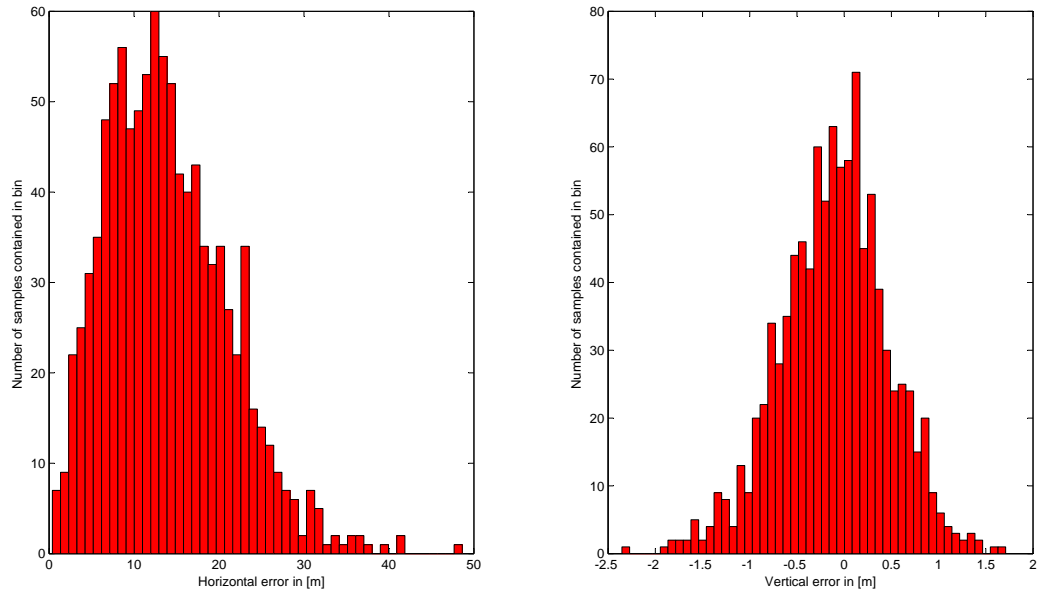Figure 3: Error propagation over time

Figure 4: Histogram plots of the errors after 20 seconds

6. INFLUENCE OF THE DIFFERENT ERROR COMPONENTS   In the following section each error source is analyzed. For this purpose only one error at the time was simulated with the above mentioned standard deviations while all others were kept at zero.

1. Influence of initial position and velocity errors
   The first values influencing the calculated trajectory are the initial position and speed. Equation (1) shows that the initial position is a constant over which is not integrated. Therefore, the introduced error is simply an additive constant but does not influence the shape of the trajectory. The initial position has a minimal influence on the latitude dependent Coriolis acceleration. However, in the order of a few meters, this value can be neglected. The simulated scenario is an approach to an airport with a GBAS station providing corrections. The resulting total position error has a standard deviation of approximately one meter.
   The situation is slightly different for initial speed information. As discussed in section 3, speed can be determined very accurately and is inaccurate only in the range of about one centimeter per second. Initial speed v_0 from equation (1) is a constant over which is integrated during the simulation time. Thus the resulting position error is linear. The maximum horizontal position error resulting from initial speed errors is just 0.26 meters, while the mean error is 0.1 meter. The errors at the end of simulation time are tested for Gaussian distribution with the Jarque-Bera test at a significance level of 5%. North, east and down component show normal distribution as expected.

2. Influence of erroneous acceleration measurements
   The next parameter influencing the trajectory is the error introduced by incorrect accelerometer measurements. Figure 5 shows the east error histogram after 20 seconds.
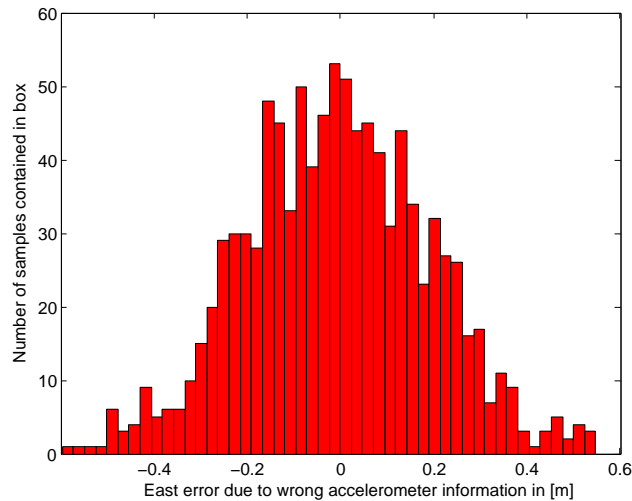

Figure 5: Histogram plot of the east errors after 20 seconds.

The maximum horizontal position error is 0.78 meters while the mean error is 0.25 meters. Thus, only a very small portion of the overall error is introduced through incorrect accelerometer data. The errors do not show linear behavior any more but increase faster since wrong information is integrated twice. As before the resulting position error from

8

the accelerometer uncertainties was investigated with the Jarque-Bera test. All three components of the error were again found to be Gaussian distributed.

3. Influence of Attitude Errors

The above results already suggest that the attitude errors are responsible for the greatest portion of the overall error. Indeed, the errors after 20 seconds simulation time caused by incorrect attitude information are almost as big as the total errors.
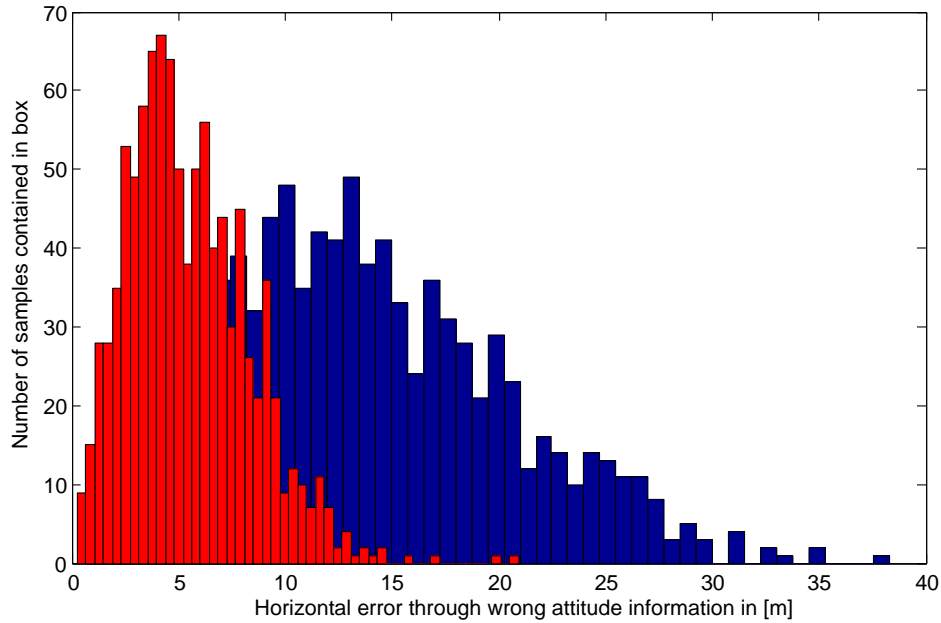

Figure 6: Histogram of errors after 20 seconds. Shown in red is the error caused by incorrect initial attitude information while in blue the errors caused by incorrect rate gyro information are plotted.

Incorrect attitude has to be separated in two different parts. One is the initial attitude estimate from GNSS measurements, the other one is the constantly updated attitude determined by rate gyro measurements. In this first consideration both measurements were modeled with their respective error behaviors. Taking a look at them separately gives some further insights. Figure 6 shows histograms of the errors after 20 seconds of simulation time. Plotted in red is the error portion caused by wrong initial attitude information while in blue the error caused by wrong gyro information is shown.

While erroneous initial attitude information causes a mean position error of 5.5 meters and a worst error of 20.9 meters, wrong gyro information has an even worse effect. The mean error in that case is 13.1 meters and the maximum error was found to be 38.3 meters. This results from the fact that turn rate information is integrated three times: for the first time when calculating the transformation matrix for the specific force and then twice to obtain speed and thereafter position information. Thus an error in turn rate information has the largest effect from all errors discussed in the preceding sections.

7. CONCLUSION AND OUTLOOK   In this paper the performance of a simple GNSS/INS integration has been investigated. Hereby a low-cost MEMS-INS is initialized with the last assured position, speed and attitude information which is derived solely from GNSS measurements. It takes over navigational responsibility after a problem with satellite navigation is detected and continues to provide safe guidance while the satellite signals are reacquired. With error models for all different sources of errors simulations show that the system performs sufficiently well for a minimum of 14.4 seconds. After this timespan the position error which is mainly driven by attitude uncertainties becomes larger than the CAT-III alert limit for GNSS navigation. However, for short term losses of GNSS signals, e.g. during turns as shown in figure 1, this method can be a very useful and cost efficient way of addressing the problem. This is especially important when limited satellite coverage prevails. In future studies an integrity concept for this architecture should be investigated to ensure safety for civil aviation.

References

[1] D. H. Titterton; J. L. Weston. *Strapdown inertial navigation technology*, volume Volume 5 of *IEE Radar, Sonar, Navigation and Avionics Series*. Peter Peregrinus Ltd. on behalf of the Institution of Electrical Engineers, 1997.

[2] Boubeker Belabbas; Patrick Rémi; Michael Meurer. Galileo Performance Assessment for CAT III GBAS. 2008.

[3] Frank van Graas; Andrey Soloviev. Precise velocity estimation using a stand-alone gps receiver. *Journal of the Institute of Navigation*, 51, No 4, Winter 2004, 2004.

[4] David De Lorenzo; Santiago Alban; Jenifer Gautier; Per Enge; Dennis Acos. GPS Attitude Determination for a JPALS Testbed: Integer Initialization and Testing. *Proceedings of the IEEE PLANS 2004*, 2004.

[5] J. Chris McMillan. A GPS Attitude Error Model for Kalman Filtering. *Defence Research Establishment Ottawa*, 1994.

[6] Demoz Gebre-Egziabher. *DESIGN AND PERFORMANCE ANALYSIS OF A LOW-COST AIDED DEAD RECKONING NAVIGATOR*. PhD thesis, Stanford University, Department of Aeronautics and Astronautics, 2004.

[7] Michael C. Mackey Andrzej Lasota. *Chaos, Fractals and Noise Stochastic Aspects of Dynamics*. Applied Mathematical Sciences 97. Springer Verlag, 1997.

[8] C. M. Jarque; A. K. Bera. A test for normality of observations and regression residuals. *International Statistical Review*, 55, 1987.